UNIVERSITI
MALAYSIA
PERLIS

Effect of Amino Acid Concentration on the Gold Nanoparticle for Calcium Phosphate Formation: UV-Vis and SEM Studies

Annisa Tsalsabila[1,2], Yuliati Herbani[1], and Yessie Widya Sari[2, *]

[1]Research Center for Photonics, National Research and Innovation Agency (BRIN), Building 442 National Science Technopark BJ Habibie, Serpong, South Tangerang, Banten 15314, Indonesia
[2]Department of Physics, Faculty of Mathematics and Natural Sciences, IPB University, Bogor 16680, Indonesia

ABSTRACT

The strong binding of amine to gold nanoparticles increases the usage of amino acids to functionalize gold nanoparticles. In this study, different charged amino acids were used as a capping agent for the gold nanoparticle to induce calcium phosphate formation. Glutamic and aspartic acid were negatively charged, while lysine and arginine were used as positively charged amino acids. The final ratio of gold to amino acid concentration (c_{Au}/c_{AA}) was 0.6 and 0.45. The variation concentration effect of amino acids in binding with gold nanoparticles was characterized using ultraviolet-visible (UV-Vis) spectroscopy. Slightly shifted in UV-Vis absorbance was recorded after gold nanoparticles were functionalized by amino acids indicating the existence of amino acids on gold nanoparticle surfaces. After being capped with amino acids, the solution of gold nanoparticles was tested using zeta potential, which showed the high stability of the solutions containing aspartic acid. Finally, the amino acid-capped gold nanoparticles solution was added by calcium and phosphate sources to form calcium phosphate. Interestingly, not all samples showed the existence of calcium phosphate formation based on scanning electron microscopy-energy-dispersive X-ray spectroscopy (SEM-EDS) results. However, the EDS results indicate that calcium phosphate was formed on the sample that contained lysine with 0.45. The results suggest that the calcium phosphate formation on amino acid-capped gold nanoparticles depends on the amino acid and the ratio concentration of gold nanoparticles to amino acids.

Keywords: Amino acids, calcium phosphate, gold nanoparticles

1. INTRODUCTION

Gold nanoparticles are widely used in various applications, including biological ones, due to their distinctive optical characteristics [1]. According to its biocompatibility and high surface volume, gold nanoparticles possess various novel applications in dentistry, such as periodontology, dental caries, and tissue engineering [2]. Organic compounds such as amines, polymers, and proteins have been widely studied as capping and reducing agents to synthesize gold nanoparticles [3]. The previous study reported amine binding was strong as thiol binding to a gold nanoparticle which motivated the researcher to use amino acids as surface modificatory for nanogold [4]. Functionalizing gold nanoparticles using amino acids has been proven to strongly affect the interaction of nanogold with cells and, when in close contact, contributes to antibacterial effects and cytotoxicity [5]. Numerous applications have been examined in the research on gold nanoparticles capped with amino acids. Asparagine has been reported as an efficient catalyst for the reductive degradation of methyl orange, rhodamine B, xylenol orange, and acid red 27 during the functionalization of gold nanoparticles [6]. Due to the simplicity of detecting a color change when arginine functionalized gold nanoparticles interact with dibutyl phthalate, their use in the measurement of dibutyl phthalate in baijiu samples has been described [7].

Aspartic acid has been investigated as a reductant and stabilizer for gold nanoparticles in the selective detection of chromium (III) ions [8]. Additionally, employing aspartic acid to functionalize gold nanoparticles can act as a template for synthesizing hydroxyapatite when added calcium and phosphate ions [9].

The roles of amino acids in biomimetic mineralization have been thoroughly researched because they are necessary components of protein [10]. Aspartic acid and glutamic acid have a carboxylate group that plays a vital role in selective modification. These two amino acids were reported to modify brushite (DCPD) to the hydroxyapatite phase [10]. Furthermore, glutamic acid, arginine, and glycine were also reported to quicken the conversion process of calcium carbonate to hydroxyapatite. Glutamic acid and arginine have a more substantial effect than glycine because they are high in carboxyl and amino groups, respectively. The carboxyl or amino can peculiarly bind to calcium and phosphate ions to facilitate hydroxyapatite formation from calcium carbonate [11]. In the study using molecular dynamics and meta-dynamics simulations, arginine residue remains in the core position to promote calcium phosphate nucleation [12].

In contrast, hydrophobic amino acids (alanine, phenylalanine, proline, and methionine) hindered the hydroxyapatite crystallization [13]. The transformation of amorphous calcium phosphate is inhibited, except for phenylalanine, according to research on the effects of various amino acids, including aspartic acid, lysine, asparagine, serine, and phenylalanine, on the production of calcium phosphate [14]. A study [14] shows that aspartic acid can shrink calcium-deficient hydroxyapatite in the (002) direction. Glutamic acid, asparagine, cysteine, glutamine, arginine, histidine, and lysine all showed a decrease in CDHA crystallite size in the (002) direction in the research of amino acids on gold nanoparticles to create hydroxyapatite in calcium-deficient conditions [15]. However, the amino acid effect on hydroxyapatite mineralization needs to be better understood. They can either encourage or hinder HA mineralization, whether dissolved in solution or bound to the surface [16]. Different experimental setups may result in varying reports on the involvement of amino acids in hydroxyapatite production.

In previous work, we synthesized CDHA on amino acid capped gold nanoparticles with a final ratio concentration of gold to amino acid (c_{Au}/c_{AA}) 0.9 [15]. This study aims to evaluate the ratio concentration of gold to amino acid (0.6 and 0.45) to induce the mineralization of calcium phosphate. Different charges of amino acids were used for gold nanoparticle functionalization, the negative charge, such as glutamic acid and aspartic acid, and the positive charge, such as arginine and lysine. The absorbance of amino acid-capped gold nanoparticles and the effect of calcium addition in the solution was recorded by UV-Vis spectroscopy. In addition, the solution stability of gold nanoparticles after being capped with amino acids was recorded by zeta potential. In the evaluation of amino acid-capped gold nanoparticles to induce calcium phosphate formation, SEM-EDS was used. The results show the final ratio of amino acid to cap gold nanoparticles influences calcium phosphate formation.

2. MATERIAL AND METHODS

2.1 Materials

Potassium gold (III) chloride (KAuCl$_4$) (Sigma-Aldrich, 98%, CAS No. 13682-61-6) was used as a gold source. The Sodium borohydride (NaBH$_4$) (Kanto Chemical Co. Inc., Japan) acted as a reducing agent. L-Aspartic acid (Asp, CAS No. 56-84-8) was acquired from Sigma Aldrich, France. L-Arginine (Arg, CAS No. 74-79-3) and L-Glutamic acid (Glu, CAS No. 56-86-0) were obtained from Sigma Aldrich, Japan. L-Lysine (Lys, CAS No. 56-87-1) was procured from Sigma Aldrich, Switzerland. All solutions were prepared in purified water by the Evoqua system. Calcium source (CaCl$_2$) and phosphate source ((NH$_4$)$_2$HPO$_4$) were provided by Merck KGaA. NaOH solutions (1 M) adjusted pH to 10 for Arg-, Lys-, and Glu-AuNPs.

2.2 Synthesis of Amino Acid Capped Gold Nanoparticles for Calcium Phosphate Formation

The reduction method of gold was done using the chemical reduction method described earlier[9] [15]. An amount of 50 mL of 0.1 mM $KAuCl_4$ was reduced by 5 mg $NaBH_4$ to form gold nanoparticles. The 45 mL gold nanoparticle solution was then capped with 5 mL amino acid. This experiment uses 4 amino acids with two different concentrations, 1.5 mM and 2 mM. These different concentrations are based on the final ratio of gold to amino acid (c_{Au}/c_{AA}) 0.6 and 0.45, respectively. The 1 M of NaOH was added to the solution to adjust pH to 10 for all samples except Asp. The pH adjustment influenced the H^+ and OH^- ions in the solutions [17]. The amino acid-capped gold nanoparticles then aged for one night. The calcium phosphate preparation was done by adding 4 mL of 10^{-2} M $CaCl_2$ to 36 mL amino acid capped gold nanoparticles under continuous stirring for 10 minutes, then aged for 1 hour. A total of 4 mL of 10^{-2} M $((NH_4)_2HPO_4)$ was added to 36 mL amino acid-capped gold nanoparticles containing Ca. The solution was stirred for 1 hour and then aged to get precipitates. Finally, it was centrifuged to separate supernatant and precipitates, followed by dried precipitates in the hot plate at 40 °C before characterization. Table 1 indicates the samples prepared in this study.

Table 1 Label of samples after calcium and phosphate addition

Amino Acids	Initial Concentration of Amino Acids	
	1.5 mM	**2 mM**
Aspartic Acid	1.5Asp	2Asp
Glutamic Acid	1.5Glu	2Glu
Arginine	1.5Arg	2Arg
Lysine	1.5Lys	2Lys

2.3 Characterization

The optical characteristic of the gold ion solution after $NaBH_4$, amino acids, and calcium source addition were studied using Ultraviolet-visible (UV-Vis) spectroscopy. The absorbance of the solution was recorded using a Maya2000 Pro spectrophotometer at 200-800 nm. Nanogold stabilization after capping with amino acids was studied using zeta potential NanoPlus particulate systems (Micromeritics, USA). The morphology and elemental characterization were performed using scanning electron microscopy–energy-dispersive X-ray spectroscopy (SEM-EDS; FEI Quanta 650). The sample was not required to be coated with gold before SEM-EDS characterization to avoid bias with the gold nanoparticles on the sample.

3. RESULTS AND DISCUSSION

3.1 UV-Vis and Zeta Potential Characterization

The chemical reduction method utilizing sodium borohydride was used to obtain gold nanoparticles. The addition of sodium borohydride to gold ion solution changed the color from yellowish transparent to ruby red solution after 20 minutes of stirring at room temperature. The ruby-red color of gold nanoparticles came from electromagnetic waves' reflection from nanoparticles [1]. In addition, the absorbance characteristic of the gold nanoparticles was monitored using UV-Vis spectroscopy. The absorbance peak of gold nanoparticles in this study ranged from 501.55 nm to 509.36 nm, which correlated with the excitation of surface plasmon vibrations of gold nanoparticles [4]. This absorbance peak was consistent with previous research showing the peak wavelength at 510 nm in gold nanoparticles obtained from borohydride reduction of aqueous chloroauric acid [4].
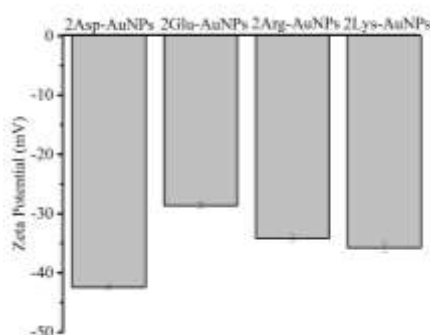
Figure 1. Zeta Potential of AA-AuNPs with AA concentration of 2 mM.
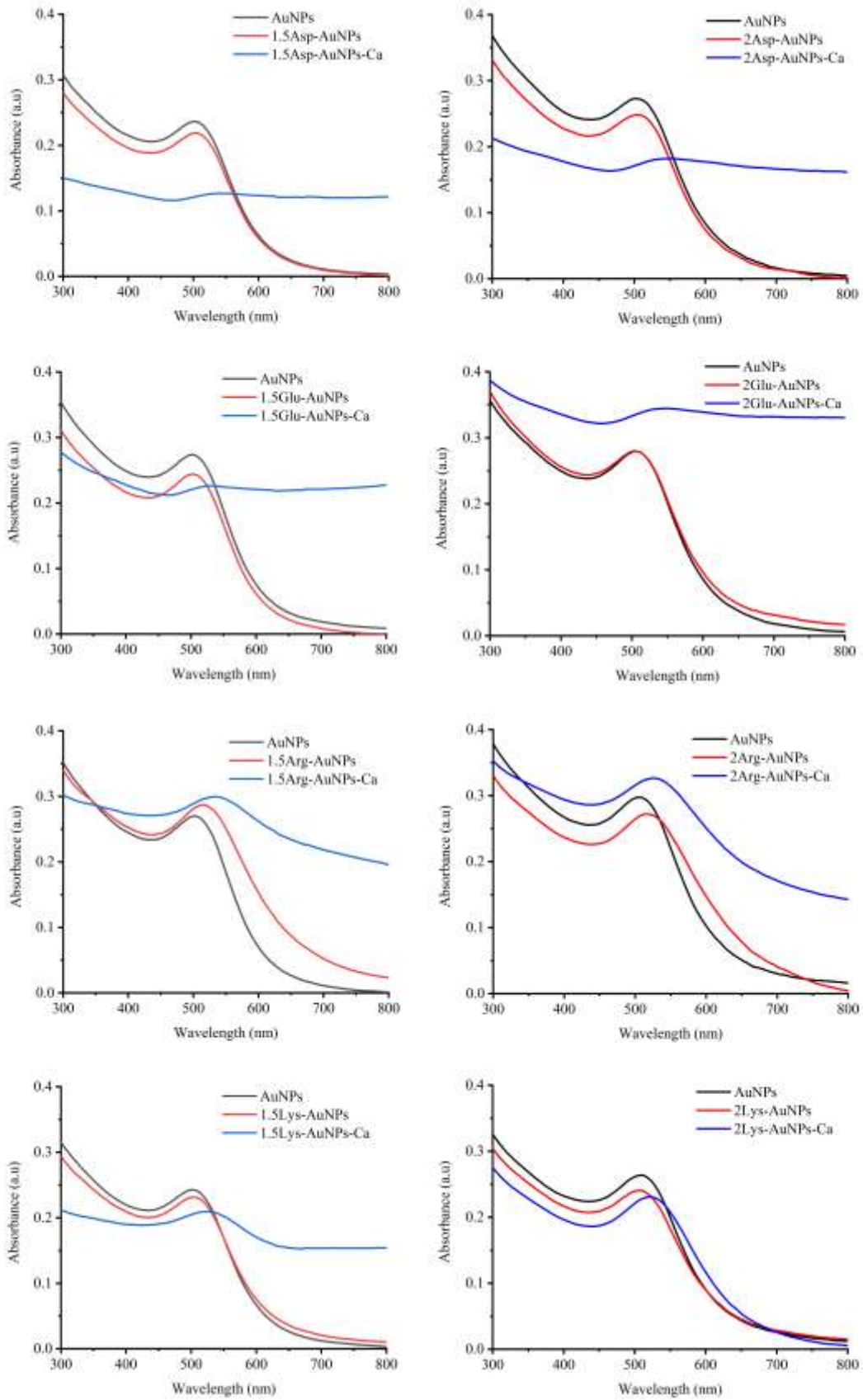
Figure 2. UV-Vis graph of the Asp, Glu, Arg, and Lys with the concentration of 1.5 mM and 2 mM on gold nanoparticles.

The addition of aspartic acid, glutamic acid, and lysine to gold nanoparticles in different concentrations did not change the color of nanogold solutions. Arginine addition to gold nanoparticle solutions resulted in the color shifting from ruby-red to purple at both concentrations, 1.5 mM and 2 mM. The ruby-red to purple hue shift indicates the nanoparticle aggregation due to particle plasmon interfacing [1]. The stability of amino acid-capped gold nanoparticles with the concentration of 2 mM was confirmed by zeta potential, which can be seen in Figure 1. The zeta potential values of all prepared samples with positive and negative charge amino acids were negative, indicating the formation of negative charge surfaces. The negative surface charge may result from the carboxylate group that remained on the outer surface of the prepared sample [6] [18]. The interaction of gold nanoparticles with amino acids results in the negative surface charge of amino acids-capped gold nanoparticles that are beneficial for preventing agglomerations and long-life stability [6]. The value of zeta potential results were -42.46 mV, -28.64 mV, -34.17 mV, and -35.75 mV for 2Asp-, 2Glu-, 2Arg-, and 2Lys-AuNPs, respectively. Due to its larger absolute value than the other samples, 2Asp-AuNPs were found to be the most stable amino-acids-capped gold nanoparticle in this experiment. A value higher than 30 mV was classified as a highly stable colloidal solution [19] [20]. In the 2Glu-AuNPs, the zeta potential value was lower than 30 mV indicating the solutions were not stable as Lys, Arg, and Asp.

Arg and Lys have been reported to bind to gold nanoparticles using the amino side chain, while the Asp and Glu will oscillate on the surface along the z-direction using carboxylic groups, based on the molecular dynamics simulation study [21]. The existence of amino acids on the gold nanoparticle surface can be confirmed by the shift in maximum wavelength on UV-Vis absorbance [22]. The effect of two different concentrations at various amino acids capped gold nanoparticles is shown in Table 2 and Figure 2. The gold nanoparticle capped with 1.5 mM amino acids showed a red shift for all amino acids, while the gold nanoparticle with 2 mM had a slightly blue shift for Glu and Lys. The red shift of Arg-capped gold nanoparticles was higher than Asp, Glu, and Lys, which also can be observed with the naked eye that the adding Arg to gold nanoparticles changed the solution to a purplish color. The broadening and redshift of surface plasmon resonance indicate the modification in the surface of gold nanoparticles after capping with amino acids [23]. The variates optical properties after amino acid-functionalized gold nanoparticles represent different stability of the solutions [5]. In the study of L-Arginine for stabilizing gold nanoparticles, an increase in Arg content caused a hypsochromic shift of the localized surface plasmon resonance peak [24].

Table 2 Peak Wavelength of AuNPs, AA-AuNPs, and AA-AuNPs-Ca

Amino acids	Peak wavelength (nm)					
	AuNPs	1.5AA-AuNPs	1.5AA-AuNPs-Ca	AuNPs	2AA-AuNPs	2AA-AuNPs-Ca
Asp	501.55	504.31	540.08	501.09	503.39	552.42
Glu	501.55	502.01	530.00	507.07	502.47	550.59
Arg	502.01	514.41	533.21	505.23	517.17	524.96
Lys	502.01	505.23	524.05	509.36	508.44	521.30

The peak wavelength after calcium addition to the amino acid-capped gold solution can be seen in Table 2, while the UV-Vis graph can be seen in Figure 2. The addition of calcium caused the UV-Vis spectrum to shift to a longer wavelength suggesting the aggregated nanoparticles [9]. In the study of gold nanoparticles with aspartic acids as a capping agent, the addition of calcium significantly shifts the UV-Vis graph due to open structures of particles and longitudinal plasmon vibrations excitation [9]. It can be seen from the graph for amino acids with positive charges, Lys and Arg, that the curve was shown the gold nanoparticle characteristics. Conversely, the amino acids with negative charges, Asp and Glu, showed an almost flat pattern. The results of this

investigation agree with the previous study in that the concentration ratio of gold nanoparticles and amino acids was 0.9 [9]. The research on arginine also reported the intensive and narrow surface plasmon resonance functionalized gold nanoparticles on apatite that indicate the uniform and highly stable nanogold [5]. On the other hand, adding calcium source to negative charge amino acid for both concentrations resulted in the broad surface plasmon resonance maxima, indicating a non-stable structure [5].

3.2 Morphological Characteristic and Elemental Composition
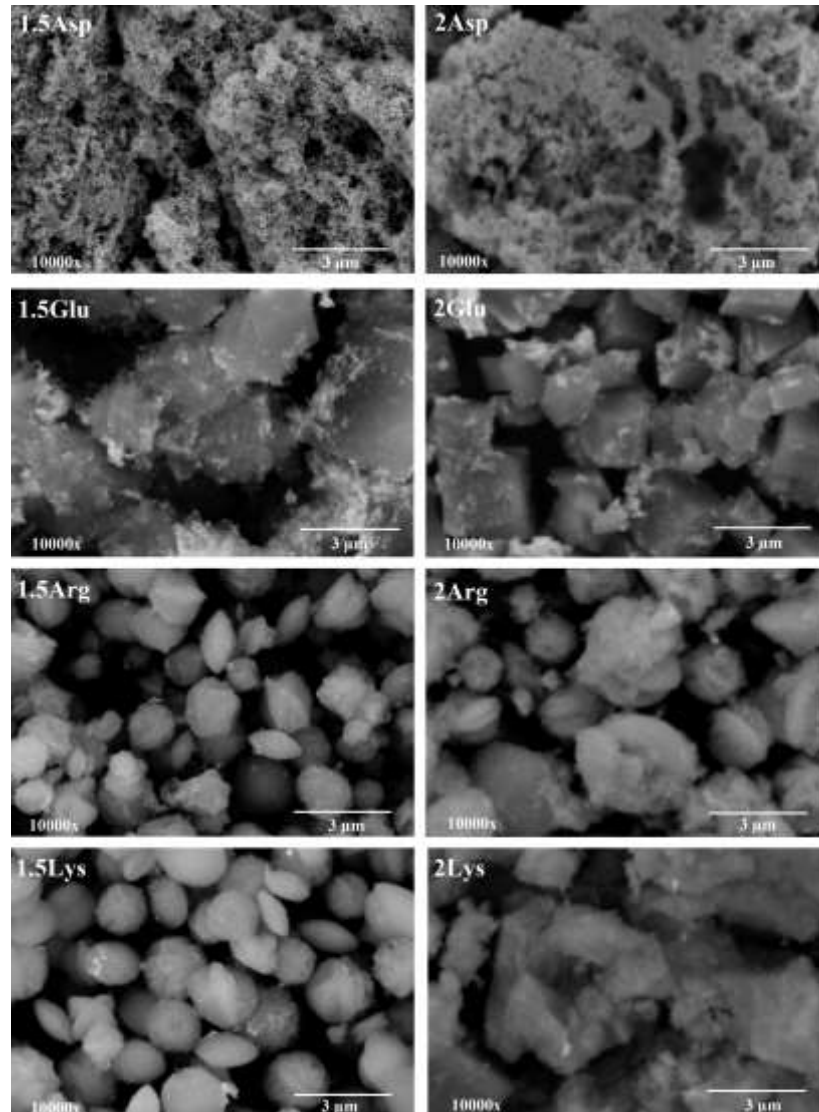
Figure 3. Morphology of the gold nanoparticle with different concentration of amino acid after calcium and phosphate addition.

Figure 3 represent the SEM image of amino acids capped gold nanoparticle after calcium and phosphate addition. In the sample that contains 1.5 mM Asp, the morphological characteristic was tiny spherical agglomerated. Moreover, increasing the Asp content to 2 mM did not change the morphological features. The elemental composition obtained from EDS results showed that Au was the highest element in both samples, 85.1 wt% and 82.4 wt%, for 1.5Asp and 2Asp, respectively. The minor components of 1.5Asp were C, N, Al, P, Cl, and K. In contrast, the minor parts of 2Asp were C, O, N, Na, Cl, Ca, P, and K. The absence of calcium and phosphate in 1.5Asp and just less than 0.5 wt% in the 2Asp indicate that the variation in concentration between 1.5 mM and 2 mM did not produce calcium phosphate. The formation of calcium phosphate was

indicated by the existence of calcium and phosphate as the main element of elemental composition. According to a prior study, the presence of Asp did not affect the crystallization of dicalcium phosphate dihydrate (DCPD) at different Asp concentrations (1,2,5, and 10 mM) [25]. On the other hand, the concentration of 1 mM of Asp on gold nanoparticles was reported to induce the formation of CDHA with needle-like morphological characteristics in the FE-SEM characterization [15]. Similarly, in the study of the hydroxyapatite formation on gold nanoparticles capping with aspartic acids, the morphology was shown quasi-spherical structure that corresponded to the hydroxyapatite pattern on X-Ray diffraction results[9].

In the 1.5Glu sample, the morphological characteristic was a cubical shape with tiny spherical agglomeration. The elemental composition was O (37.8%), Ca (23.2%), C (18%), Au (16.4%), N, P, Na, and Cl. In increasing Glu content to 2 mM, the elemental composition was O (30.7%), Ca (29.9%), Au (22.7%), C (15.9%), Na, P, and Cl. The morphology of 2Glu was a cubical shape smaller than 1.5Glu. The presence of P as a smaller element in the 1.5Glu and 2Glu sample indicate these two-sample did not induce calcium phosphate formation. The bright tiny spherical agglomerated may be contributed by Au. It has been reported in the previous study about the composite of gold and hydroxyapatite, the gold morphology was seen as brighter than hydroxyapatite because reflected electrons from Au as heavy elements are more abundant than light elements such as Ca and P [26]. The cubical shape can be identified as CaO since the major element that appears are Ca and O besides Au. The cubical shape of CaO was also identified by other researchers who synthesized CaO from Mollusc shells [27].

The morphology of the 1.5Arg sample was oval and sphere with O (34.4%), C (26.8%), Ca (18.9%), Au (18.2%) as major elements, and P, Na, Sc, and Cl as minor elements. Similarly, the 2Arg sample also had oval and sphere forms. The primary component of 2Arg was O (29.6%), Ca (27%), Au (24%), and C (14.1%), whereas F, P, and Na appeared as minor elements. The detected P was less than 10wt% in both samples indicating that 1.5Arg and 2Arg did not consider suitable for calcium phosphate growth. Furthermore, the variation concentration of Arg from 1.5 mM to 2 mM did not induce calcium phosphate formation. In the previous report, Arg has an inhibitory effect on the hydroxyapatite nucleation, whereas Glu has an inhibitory effect on crystal growth [28].

The oval form was seen in 1.5Lys with the major elements O (35.9%), Ca (22.2%), Au (21.3%), C (17.9%), and N, P, Na, and Cl as minor elements. The small P content (less than 1 wt%) indicates that calcium phosphate was not formed on the sample. Interestingly, the addition of Lys at a concentration of 2 mM has induced the calcium phosphate formation with the primary element Ca, Au, O, and P, respectively. The Ca/P ratio of the 2Lys sample was 2.19, matching the range of amorphous calcium phosphate between 1.2 and 2.2 [29]. The morphological shape of 2Lys was seen to be aggregated. In the previous study, 1 mM lysine was reported to induce CDHA formation with a smooth needle-like formation and Ca/P ratio of 1.41 [15]. Therefore, it can be concluded that the production of calcium phosphate in this study only forms in the sample that contains 2 mM of Lys.

4. CONCLUSION

In summary, gold nanoparticle was obtained using chemical reduction methods with an absorbance peak of 502 to 509 nm. Four different amino acids with two different concentrations were used for gold nanoparticle functionalization. Asp was the most stable solution of amino acids capped gold nanoparticles at a concentration of amino acids of 2 mM, followed by Lys, Arg, and Glu. Variation of amino acid concentration led to a shift peak wavelength on UV-is spectroscopy. Asp, Arg, and Glu at concentrations of 1.5 mM and 2 mM prevented the formation of calcium phosphate after calcium and phosphate addition. In the presence of 2 mM of Lys on the gold nanoparticle, the calcium and phosphate addition has influenced the calcium phosphate formation, as indicated by the elemental composition of EDX. The results suggest that the calcium

phosphate on amino acid-capped gold nanoparticles depends on the amino acid and the ratio concentration of gold nanoparticles to amino acids.

ACKNOWLEDGEMENTS

REFERENCES

[1]   V. A. Ogarev, V. M. Rudoi, and O. V Dement'eva. Inorg. Mater. Appl. Res. vol. 9, no. 1, (2018) pp. 134–140.
[2]   R. A. Bapat et al. Int. J. Pharm., vol. 586, (2020) p. 119596.
[3]   T. Maruyama, Y. Fujimoto, and T. Maekawa. J. Colloid Interface Sci. vol. 447, (2015) pp. 254–257.
[4]   S. Mandal, S. Phadtare, and M. Sastry. Curr. Appl. Phys. vol. 5, no. 2, (2005) pp. 118–127.
[5]   M. Vukomanovic, M. del M. Cendra, A. Baelo, and E. Torrents. Colloids Surfaces B Biointerfaces. vol. 208, (2021) p. 112083.
[6]   N. Garg, S. Bera, L. Rastogi, A. Ballal, and M. V Balaramakrishna. Spectrochim. Acta Part A Mol. Biomol. Spectrosc. vol. 232, (2020) p. 118126.
[7]   Y. Yan, Y. Qu, R. Du, W. Zhou, H. Gao, and R. Lu. Anal. Methods. vol. 13, no. 43, (2021) pp. 5179–5186.
[8]   X. Wang, X. Wang, J. Liu, K. Wang, R. Zhao, and S. Yang. Microchem. J. vol. 159, (2020) p. 105359.
[9]   D. Rautaray, S. Mandal, and M. Sastry. Langmuir. vol. 21, no. 11, (2005) pp. 5185–5191.
[10]   X. Chu et al., J. Phys. Chem. B. vol. 115, no. 5, (2011) pp. 1151–1157.
[11]   S. Yanyan, W. Guangxin, S. Guoqing, W. Yaming, L. Wuhui, and A. Osaka. RSC Adv. vol. 10, no. 61, (2020) pp. 37005–37013.
[12]   X. Tan, Z. Xue, H. Zhu, X. Wang, and D. Xu. Cryst. Growth Des. vol. 20, no. 7, (2020) pp. 4561–4572.
[13]   S. Koutsopoulos and E. Dalas. Langmuir. vol. 16, no. 16, (2000) pp. 6739–6744.
[14]   I. Erceg et al.Crystals. vol. 11, no. 7 (2021).
[15]   Y. W. Sari, A. Tsalsabila, N. Darmawan, and Y. Herbani. Ceram. Int. vol 48, issue 10 (2022) pp. 13665-13675.
[16]   M. Tavafoghi and M. Cerruti. J. R. Soc. Interface. vol. 13, (2016).
[17]   S. López-Ortiz et al. J. Nanomater.(2020) p. 5912592.
[18]   A. Tsalsabila, Y. Herbani, and Y. W. Sari. J. Phys. Conf. Ser. vol. 2243, no. 1, (2022) p. 12102.
[19]   Z. Sun, Z. Cui, and H. Li. Sensors Actuators B Chem. vol. 183, (2013) pp. 297–302.
[20]   I. V Safenkova, E. S. Slutskaya, V. G. Panferov, A. V Zherdev, and B. B. Dzantiev. J. Chromatogr. A. vol. 1477, (2016) pp. 56–63.
[21]   F. Ramezani, M. Amanlou, and H. Rafii-Tabar. Amino Acids. vol. 46, no. 4, (2014) pp. 911–920.
[22]   C. Liu, Y. Miao, X. Zhang, S. Zhang, and X. Zhao. Microchim. Acta. vol. 187, no. 6, (2020) p. 362.
[23]   H. Joshi, P. S. Shirude, V. Bansal, K. N. Ganesh, and M. Sastry. J. Phys. Chem. B. vol. 108, no. 31, (2004) pp. 11535–11540.
[24]   A. Sunatkari, S. Talwatkar, Y. Tamgadge, and G. Muley. Nanosci. Nanotechnol. vol. 5, (2015) pp. 30–35.
[25]   K. Rubini, E. Boanini, and A. Bigi. J. Funct. Biomater. vol. 10, no. 1, (2019).
[26]   Y. Chai, M. Nishikawa, and M. Tagaya. Adv. Powder Technol. vol. 29, no. 5, (2018) pp. 1198–1203.

[27] S. Thakur, S. Singh, and B. Pal. Fuel Process. Technol. vol. 213, (2021) p. 106707.
[28] M. T. Jahromi, G. Yao, and M. Cerruti. J. R. Soc. Interface. vol. 10, no. 80, (2013) p. 20120906.
[29] S. V Dorozhkin. Biomatter. vol. 1, no. 2, (2011) pp. 121–164.